THE AMERICAN SOCIETY OF MECHANICAL ENGINEERS
345 E. 47th St., New York, N.Y. 10017

94-GT-143

ENDWALL AND UNSTEADY FLOW PHENOMENA IN AN AXIAL TURBINE STAGE

H. E. Gallus and J. Zeschky
RWTH Aachen
Aachen, Germany

C. Hah
NASA Lewis Research Center
Cleveland, Ohio

ABSTRACT

Detailed experimental and numerical studies have been performed in a subsonic, axial-flow turbine stage to investigate the secondary flow field, the aerodynamic loss generation, and the spanwise mixing under a stage environment. The experimental study includes measurements of the static pressure distribution on the rotor blade surface and the rotor exit flow field using three-dimensional hot-wire and pneumatic probes. The rotor exit flow field was measured with an unsteady hot-wire probe which has high temporal and spatial resolution. Both steady and unsteady numerical analyses were performed with a three-dimensional Navier-Stokes code for the multiple blade rows. Special attention was focused on how well the steady multiple-blade-row calculation predicts the rotor exit flow field and how much the blade interaction affects the radial distribution of flow properties at the stage exit. Detailed comparisons between the measurement and the steady calculation indicate that the steady multiple-blade-row calculation predicts the overall time-averaged flow field very well. However, the steady calculation does not predict the secondary flow at the stage exit accurately. The current study indicates that the passage vortex near the hub of the rotor is transported toward the mid-span due to the blade interaction effects. And, the structure of the secondary flow field at the exit of the rotor is significantly modified by the unsteady effects. The time-averaged secondary flow field and the radial distribution of the flow properties, which are used for the design of the following stage, can be predicted more accurately with the unsteady flow calculation.

Nomenclature

C_1	Constant in turbulence closure models
C_2	Constant in turbulence closure models
C_3	Constant in turbulence closure models
C_4	Constant in turbulence closure models
c_μ	Constant in turbulence closure models
h	Span
k	Turbulent kinetic energy
M	Mach number
p	Pressure
Pt	Total pressure
Re	Reynolds number
T	Temperature
Tu	Turbulence intensity
U, V, W	Mean velocity components
u, v, w	Fluctuating velocity components

Greek Symbols

β	Relative flow angle
ϵ	Turbulence dissipation rate
μ	Viscosity
ν	Kinematic viscosity
ρ	Density

Subscripts

0	Stator inlet condition
1	Rotor inlet condition
2	Rotor exit condition
eff	Effective value

INTRODUCTION

Modern design of advanced gas turbines requires increased aerodynamic efficiency with fewer components. To achieve maximum aerodynamic efficiency with highly loaded blade rows, an accurate understanding of the secondary flow field and boundary layer development has become essential for aerodynamic designers. In the past decade, great progress has been made in understanding the flow physics inside a blade row and developing appropriate prediction models. Various numerical methods based on steady, three-dimensional, Reynolds-averaged Navier-Stokes equations have been sufficiently developed so that these

Presented at the International Gas Turbine and Aeroengine Congress and Exposition
The Hague, Netherlands — June 13–16, 1994
This paper has been accepted for publication in the Transactions of the ASME
Discussion of it will be accepted at ASME Headquarters until September 30, 1994

tools are routinely used for the optimization of turbomachinery blade rows under design environments(Davis et al., 1988; Dawes, 1986; Denton,1986; Giles,1988; Hah,1987;etc).

Although steady isolated-blade-row analyses are very valuable for turbomachinery design, the flow field in a turbomachine is inherently unsteady as a result of the relative motion of the blade rows. As the axial gap between blade rows is reduced for compact design, the influence of the adjacent blade rows becomes increasingly important for the flow analysis of any specific blade row. A rather simple steady state multiple-blade-row calculation procedure, which employs a mixing plane concept, has been proposed to account for some of the adjacent blade row effects and to provide more consistent flow conditions for the analysis of specific blade rows in a multi-stage configuration (Arts, 1985;Dawes, 1986;Denton and Singh, 1979;Ni, 1989; etc.). This simple steady approach for the solution of multiple-blade-rows seems to give surprisingly good steady or time-averaged solutions for many flow fields (for example, W.W. Copenhaver et al., 1993) and is used widely for the optimization of multiple blade rows. With a steady multiple-blade-row calculation, mixing planes are introduced between blade rows to establish steady boundary conditions for the adjacent blade rows and any true unsteady interaction effects are not modeled. Theoretically, if the blade interaction has little effect on the time-averaged flow field, the numerical results based on this approach should be accurate enough for aerodynamic design optimization.

The interaction between the stator and the rotor flow fields in a typical turbine stage has been known to affect aerodynamic efficiency, heat transfer, and loss generation. The unsteady interaction between the stator and the rotor flow fields can be divided into the following three forms. The potential flow fields of the two blade rows affect pressure distributions on the blade surfaces and the flow angles at the inlet of the rotor (Hunter, 1982;Joslyn and Dring, 1983). In addition to the potential flow field interaction, the unsteady wake of the stator passing through the rotor has a great influence on the flow and heat transfer of the rotor (Meyer,1958; Kerrebrock and Mikolajczak, 1970;Hodson, 1983;Dring et al., 1982;etc.). The potential flow interaction and the wake interaction have been studied extensively and a wide range of experimental and analytical studies have been reported (Gallus et al., 1982) . The third form of rotor-stator interaction is due to the convection of stator secondary vortices into the rotor flow field (Binder, 1985).

Recent improvements in high-response measurement techniques and numerical techniques provide means for experimental and analytical investigations of blade interactions. The current work is focused on studying the effects of blade row interactions in a single stage turbine on the time averaged flow field. For the design of multiple turbine stages, accurate assessment of time-averaged flow conditions (static pressure,temperature, exit flow angle, etc.) are necessary at the exit of each blade row. Previous studies indicate that stage exit flow conditions are not predicted well with the steady approach. In particular, the flows underturning and overturning near the hub are not modelled properly when the blade loading is increased. The present work is aimed at studying how well a steady stage calculation procedure predicts the time-averaged flow characteristics of a single stage turbine. The numerical results are compared with measurements. Furthermore, an unsteady calculation is presented to verify that the major effects of blade row interactions on the steady flow field can be successfully calculated with the current steady calculation method. Further studies are proposed, using some of the results of the unsteady calculation, for the improvement of the current steady stage calculation method.

TEST FACILITY AND INSTRUMENTATION

The experiment was carried out in a single stage axial turbine shown in Fig. 1. For the stator, the Traupel profile is used (Utz, 1972). A modified VKI-profile is used for the rotor. Both the stator and the rotor consist of untwisted blades for the convenience of measurement of three-dimensional unsteady flow fields. A cross section of the stage with mid-span velocity triangles is shown in Fig. 2. Some of the results from the current turbine stage configuration might be specific to the current stage. However, the detailed unsteady flow data represent typical characteristics of turbine stage flow. The data, along with the numerical results, can improve the understanding of the complex flow physics in modern multi-stage turbines.

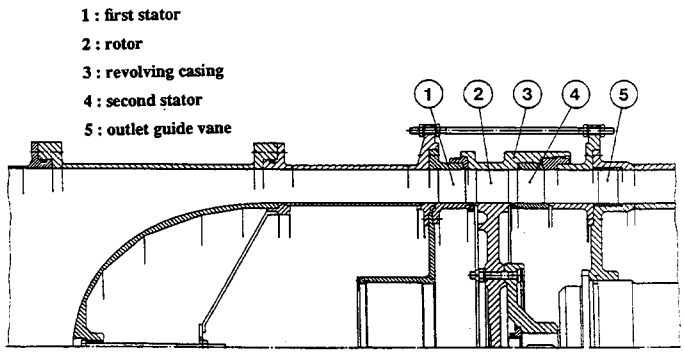

Fig. 1. Turbine test facility

The experiment was conducted in a continuous environment. The total temperature at the turbine inlet was maintained in the range of 308 K +0.5 degrees by cooling the air. The shaft speed variation was less than 0.2 percent. The Reynolds numbers were constant with an accuracy of 1.0 percent. The flow was surveyed with a pneumatic five hole probe , three-wire hot-wire probes, and a laser velocimeter. Also, a pneumatic boundary layer probe and a two-wire hot-wire probe were used near the endwall. The static pressure distribution on the rotor blade was measured with a rotating scanivalve. Miniature high response pressure transducers were mounted at 25 axial locations in the casing above the rotor to measure unsteady static pressures on the casing. The averaged absolute Mach number at the inlet of the rotor is approximately 0.45. The details of the calibration of the various probes and the data reduction for the steady and unsteady measurements are given by Zeschky and Gallus, 1993.

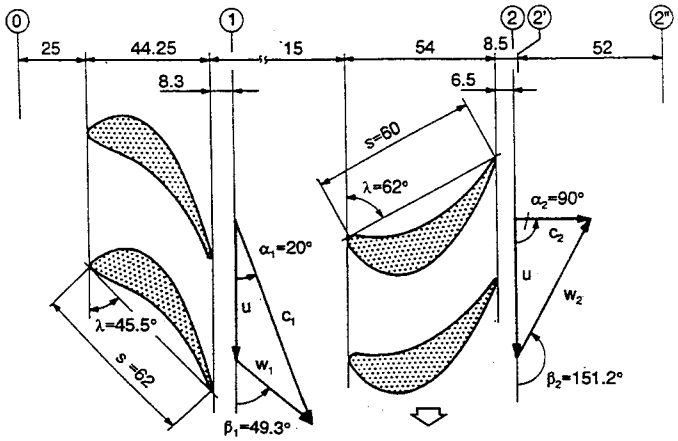

aspect ratio h/s	0.887	0.917
pitch (midspan) t	47.6 mm	41.8 mm
blade number	36	41
Reynolds number, based on chord and exit velocity	6.8×10^5	4.9×10^5
rotational speed	---	3500 rpm
tip diameter	600 mm	600 mm

Fig. 2. Turbine geometry and design data

NUMERICAL METHOD

The following Reynolds-averaged Navier-Stokes equations are solved for the current problem.

$$\frac{\partial \rho}{\partial t} + \frac{\partial}{\partial x_i}(\rho U_i) = 0 \qquad (1)$$

$$\frac{\partial(\rho U_i)}{\partial t} + \frac{\partial}{\partial x_j}(\rho U_i U_j) + 2\rho\varepsilon_{ijk}\Omega_j U_k = -\frac{\partial p}{\partial x_i} + \frac{\partial}{\partial x_j}\left[\mu\left\{\frac{\partial U_i}{\partial x_j} + \frac{\partial U_j}{\partial x_i} - \frac{2}{3}\frac{\partial U_k}{\partial x_k}\delta_{ij}\right\} - \rho\bar{u}_i\bar{u}_j\right] + F_i \qquad (2)$$

$$\frac{\partial(\rho e)}{\partial t} + \frac{\partial}{\partial x_j}(\rho U_j e) = \frac{\partial}{\partial x_j}\left[\frac{\mu}{Pr}|_{eff}\frac{\partial T}{\partial x_j}\right] - \frac{\partial}{\partial x_j}(pU_j) + U_i F_i + \frac{\partial}{\partial x_j}\left[U_i\mu\left\{\frac{\partial U_i}{\partial x_j} + \frac{\partial U_j}{\partial x_i} - \frac{2}{3}\frac{\partial U_k}{\partial x_k}\delta_{ij}\right\}\right] \qquad (3)$$

$$p = \rho RT \qquad (4)$$

where U_i = mean velocity, u_i = fluctuation velocity, e = total energy, Ω_i = angular velocity,

$$\frac{\mu}{Pr}|_{eff} = \frac{\mu}{Pr}|_{laminar} + \frac{\mu}{Pr}|_{turbulent}$$

and

$$e = C_v T + \frac{1}{2}U_i U_j$$

Any instantaneous flow variable can be split into three components: the time-averaged component, the periodic fluctuation due to the motion of the rotor relative to the stator frame, and the turbulent fluctuation. The sum of the first two parts is the phase-averaged value which is a function of time and space. The effects of the turbulent fluctuation are included through the turbulence model. The turbulence is represented through the ensemble-averaged turbulence kinetic energy and the turbulence dissipation rate. These two turbulence variables are obtained by solving unsteady semi-empirical transport equations.

$$\frac{\partial(\rho k)}{\partial t} + \frac{\partial(\rho U_i k)}{\partial x_i} = \frac{\partial}{\partial x_i}\left[\frac{\mu_{eff}}{\sigma_k}\frac{\partial k}{\partial x_i}\right] - \rho\bar{u}_i\bar{u}_j U_{ij} - \rho\varepsilon - \frac{2\mu k}{\rho^2} \qquad (5)$$

$$\frac{\partial(\rho\varepsilon)}{\partial t} + \frac{\partial(\rho U_i \varepsilon)}{\partial x_i} = \frac{\partial}{\partial x_i}\left[\frac{\mu_{eff}}{\sigma_\varepsilon}\frac{\partial \varepsilon}{\partial x_i}\right] - C_1\frac{\rho\varepsilon}{k}(\bar{u}_i\bar{u}_j U_{ij}) - \frac{\rho\varepsilon}{k}\left[C_2 f\varepsilon + \frac{2\nu k e^{-C_4 u_* l/\nu}}{l^2}\right] \qquad (6)$$

where

$$\mu_{eff} = \mu + C_\mu(k^2/\varepsilon)[1 - exp(-C_3 u_* l/\nu)]$$

and

$$f = 1 - \frac{0.4}{1.8}e^{-(k^2/6\nu\varepsilon)^2}$$

No attempt was made to optimize constants of the turbulence modeling equations for this study. Therefore, standard values of various constants of the turbulence model are used: the values are

$$C_\mu = 0.09, C_1 = 1.35, C_2 = 1.8, \sigma_k = 1.0,$$
$$\sigma_\varepsilon = 1.3, C_3 = 0.00115, C_4 = 0.5$$

Two numerical methods were applied to analyze the flow inside the current turbine stage. Although the flow inside any turbine stage is inherently unsteady due to blade row interaction, the present design system is based on the time-averaged flow field. The current study is aimed at examining how well numerical methods simulate the time-averaged flow field. Previous studies (for example, Copenhaver et al., 1993; Saxer and Giles,1993) have indicated that the steady multiple-blade-row calculation approach predicts the time-averaged flow field at the exit of the given stage very well. Therefore, the steady multiple-blade-row calculation was performed first for the present turbine stage and the numerical results were analyzed and compared with the measured data. The comparison between the measurements and the steady stage calculation indicated that the steady multiple-blade-row calculation procedure predicts the time-averaged flow field very well across the turbine stage. The only significant shortcomings of the steady approach for practical design applications were in the calculated secondary flow field at the exit of the rotor and the spanwise distribution of the stage exit flow angle (Zeschky and Gallus, 1993). To investigate these discrepancies between the time-averaged measurement and the steady stage calculation, a time accurate calculation was performed for the stage. In the following, the two numerical approaches are briefly described.

In the steady multiple-blade-row calculation, the stator and the rotor flow fields are calculated simultaneously. The inflow

condition for the stage is specified at the stator inlet and the outflow condition is specified at the rotor exit. To maintain steady flow conditions, mixing planes are established at the trailing edge of the stator and the leading edge of the rotor. At these mixing planes, circumferential variations of the flow variables are assumed to be mixed out and only radial variations are assumed to exist. The mixing analysis based on the work of Dring and Spear, 1991, is used at the mixing planes. Further details of this procedure are given by Copenhaver et al., 1993. In the current steady stage flow calculation, any unsteady effects on the time-averaged flow field are not represented in the numerical solution.

The unsteady flow calculation was performed to examine the main effects of the blade row interaction on the time-averaged flow field, especially on the secondary flow field at the exit of the stage. The ensemble-averaged flow variables in the current unsteady flow field can be efficiently obtained by coupling the time-dependent stator flow with the time-dependent rotor flow. Therefore, the two flow fields are solved with coupled time-dependent interface boundary conditions. As shown in the computational grid (Figure 3), an interface is used to transmit flow conditions between two zones. A sliding over-laid grid is used for the present application. A three-dimensional steady Navier-Stokes code which has been successfully tested for a wide range of turbomachinery flows (Hah, 1983) was extended to execute time accurate calculations. During the development, it was found that high-order discretization schemes are necessary in both space and time to avoid excessive numerical dissipation. For the time-dependent terms, an implicit second-order scheme is used. The details of the numerical procedure of the unsteady flow calculation are explained by Hah et al., 1993.

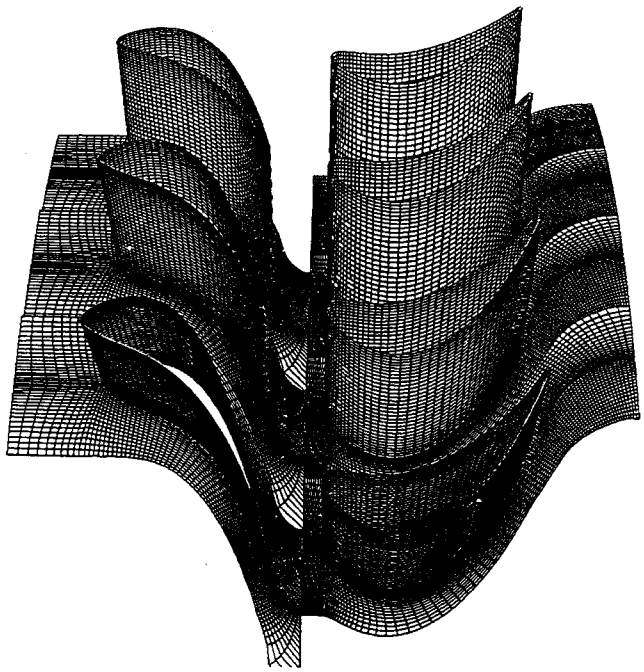

Fig. 3. Computational grid for the turbine stage

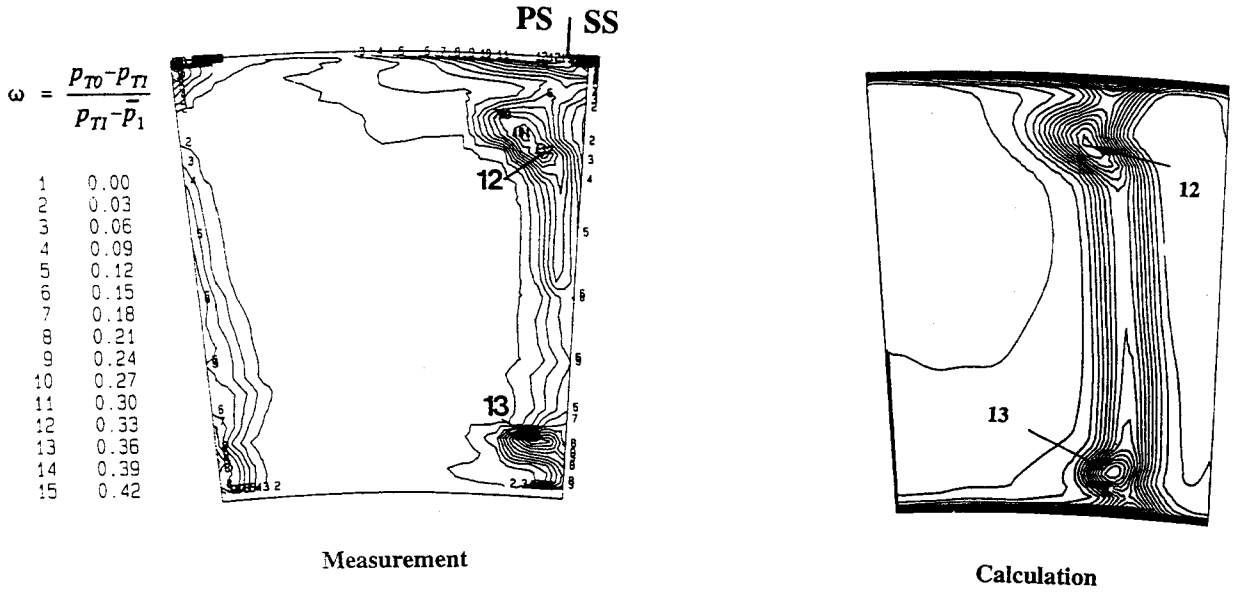

Fig. 4. Comparison of total pressure contours at stator exit

RESULTS AND DISCUSSION

Fig. 4 shows a comparison of the total pressure distribution at the exit of the stator. Both measured and calculated results are presented for one stator blade passage. Note that in Fig. 4, the circumferential locations of the domain are not matched between the measurement and the calculation. The calculated aerodynamic loss distribution matches very well with the mea-

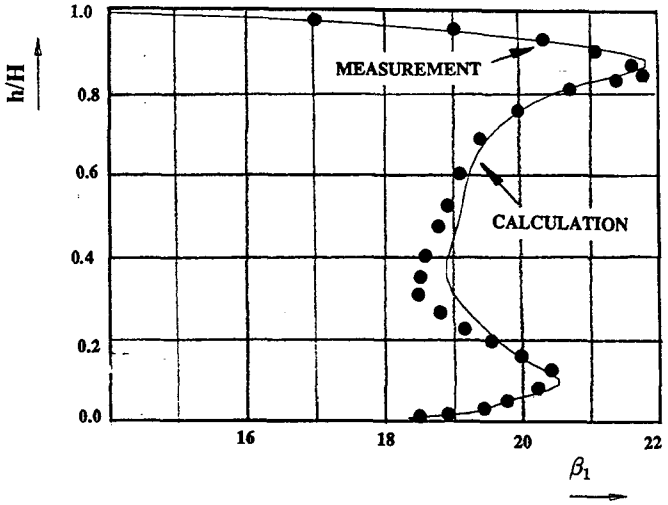

Fig. 5. Comparison of stator exit flow angle

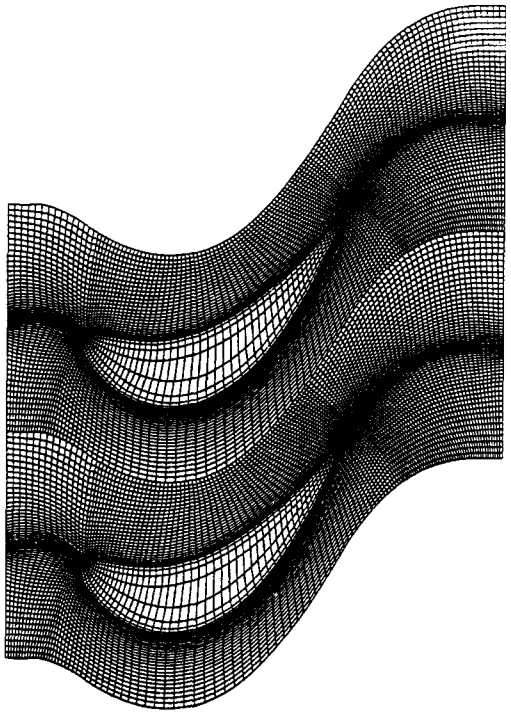

Fig. 7. Computational grid inside the tip-clearance

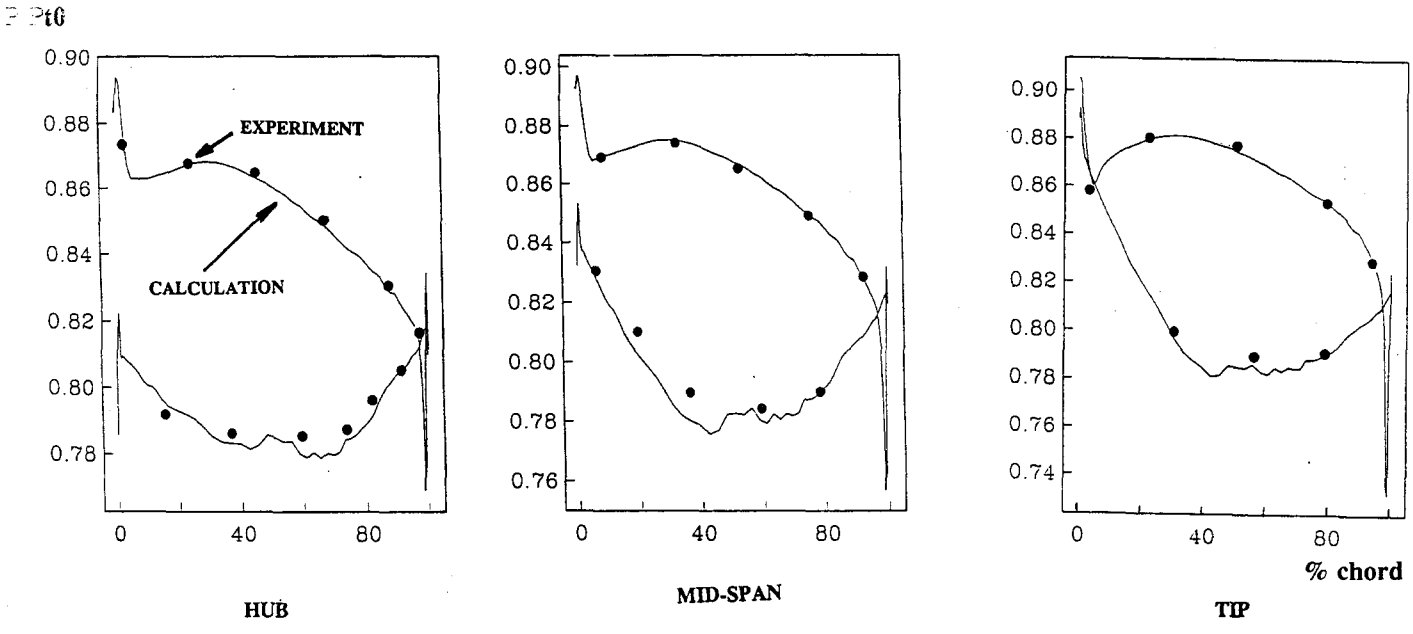

Fig. 6. Comparison of static pressure distribution on the rotor blade

surement. The radial distribution of the flow angle at the exit of the stator is compared in Fig. 5. Again, the numerical results from the steady multiple-blade-row calculation represent the overall stator flow field very well. As no other measurements were made for the stator flow field, no further comparisons are presented. The comparisons in Figs. 4 and 5 indicate that the time-averaged stator flow field is adequately calculated with the current steady stage calculation and the time-averaged inflow to the rotor is also properly modeled.

The calculated time-averaged static pressure distribution on the rotor blade is compared in Fig. 6. Because of the blade row interaction, the static pressure distribution on the rotor blade changes periodically. However, the time-averaged blade loadings are adequately calculated with the steady stage calculation. The good agreement between the steady stage calculation and the measurements in Fig. 6 is not particularly surprising. Previous studies have also shown that the steady calculation predicts time-averaged loadings very well when proper boundary conditions are used. Unsteady effects on the time-averaged loading are relatively small even in transonic turbine stages.

The detailed static pressure distribution on the endwall was measured with high response pressure transducers mounted on the endwall. The current calculation was performed with a computational grid distributed across the top of the blade tip in order to calculate the details inside the gap. Fig. 7 shows the detailed grid inside the tip gap. Ten nodes are distributed from the suction surface of the blade to the pressure side and ten nodes are clustered spanwise inside the clearance. Comparison of the static pressure distribution on the endwall between the measurement and the calculation is given in Fig. 8. Both the

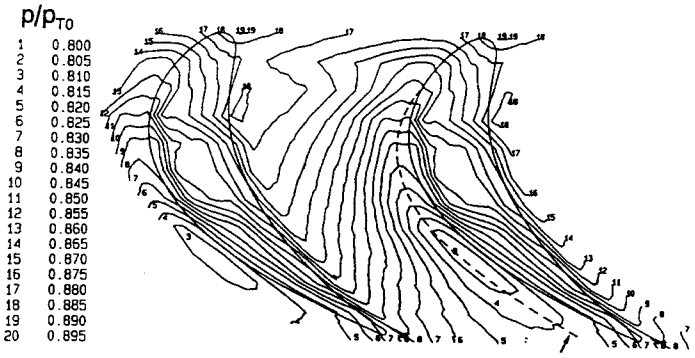

Measurement

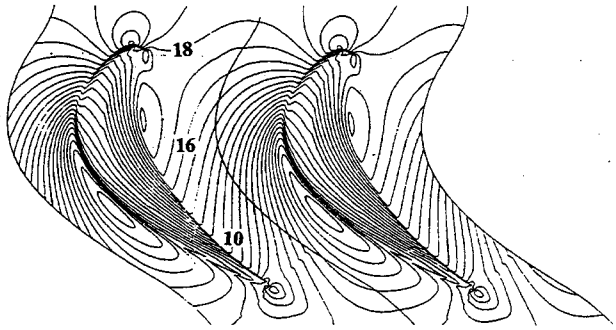

Calculation

Fig. 8. Comparison of endwall static pressure distribution

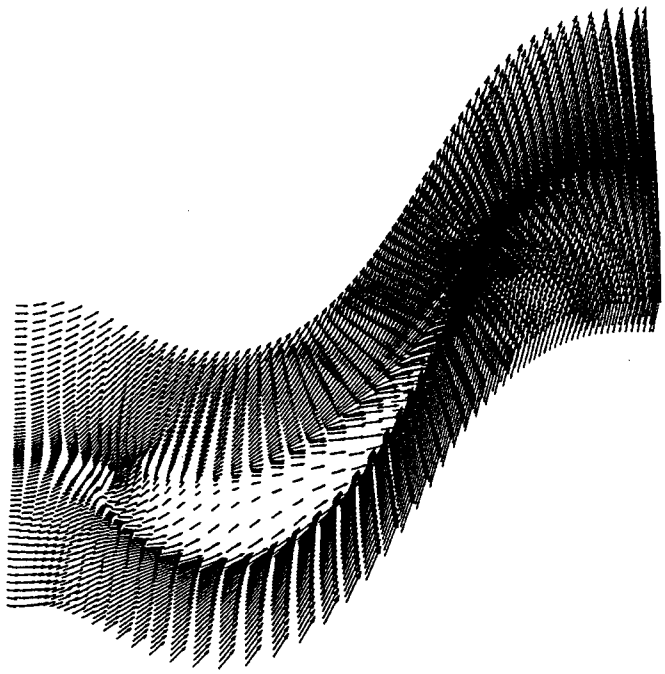

Fig. 9. Calculated velocity vectors inside the tip-clearance

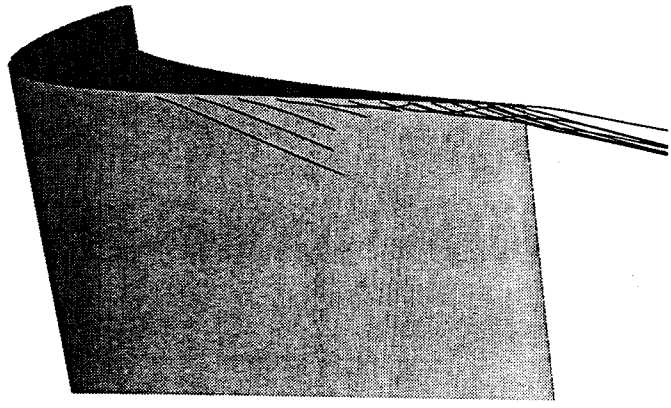

Fig. 10. Particle traces near the suction surface (tip-vortex)

measurement and the calculation show the formation of the tip clearance vortex near the suction surface toward to the trailing edge. Again, the steady stage procedure calculates the time-averaged static pressure distribution very well.

The calculated velocity vectors over the tip inside the tip gap are given in Fig. 9. The velocity vectors near the shroud show the formation of the tip vortex in more detail. Simpler numerical approaches for the tip clearance effects, using wedge-type treatments of the tip geometry, probably calculate the gross effects of the tip clearance flow on the main passage flow. However, the strength and the location of the tip vortex can not be accurately simulated without actually modeling the exact tip blade geometry. Particle traces from the numerical solution are given in Fig. 10 to show a three-dimensional view of the tip clearance vortex. Fig. 10 indicates that the tip-clearance vortex is formed very close to the shroud due to the very tight clearance (0.6 percent chord).

The secondary flow fields at the exit of the rotor are compared between the steady stage calculation and the time-averaged measurement in Fig. 11. The measured results are for two rotor blade passages while the calculated results are across one rotor blade passage. The overall structure of the flow is calculated reasonably well. However, the calculated center of the passage vortex near the hub is located at roughly 15 percent of the span compared to about 30 percent of the span from the measurement. Different sizes of the computational grid were used to analyze the prediction of this hub vortex. The numerical results from a much finer computational grid did not indicate any improvement of the location of the calculated vortex near the hub. Therefore, it was concluded that this disagreement is not due to the inadequate size of the computational grid.

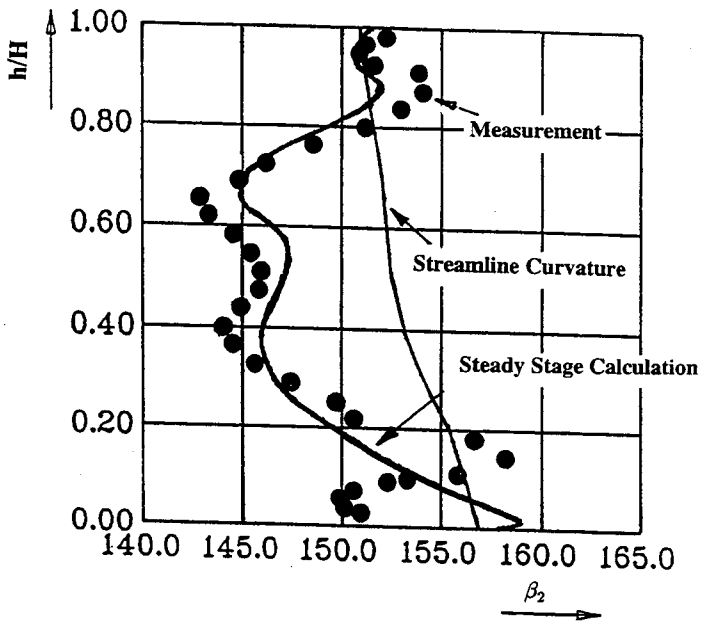

Fig. 12. Comparison of radial distribution of stage exit flow angle

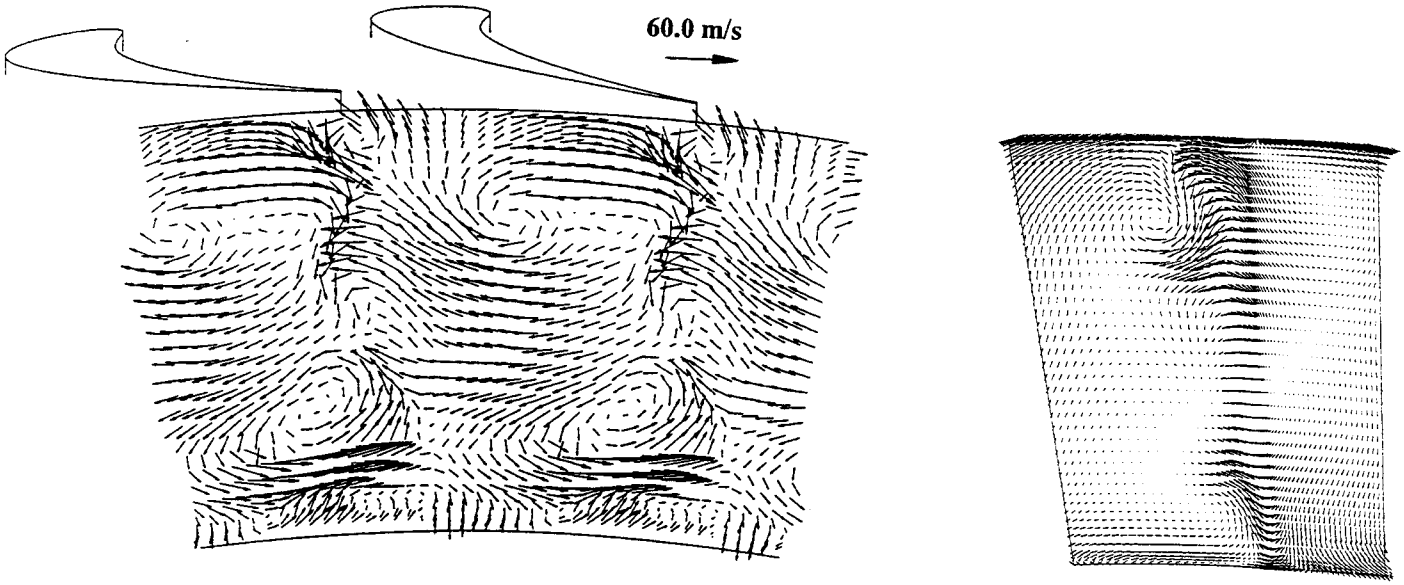

Fig. 11. Comparison of time-averaged secondary velocity at rotor exit

(velocity vectors in rotor relative frame).

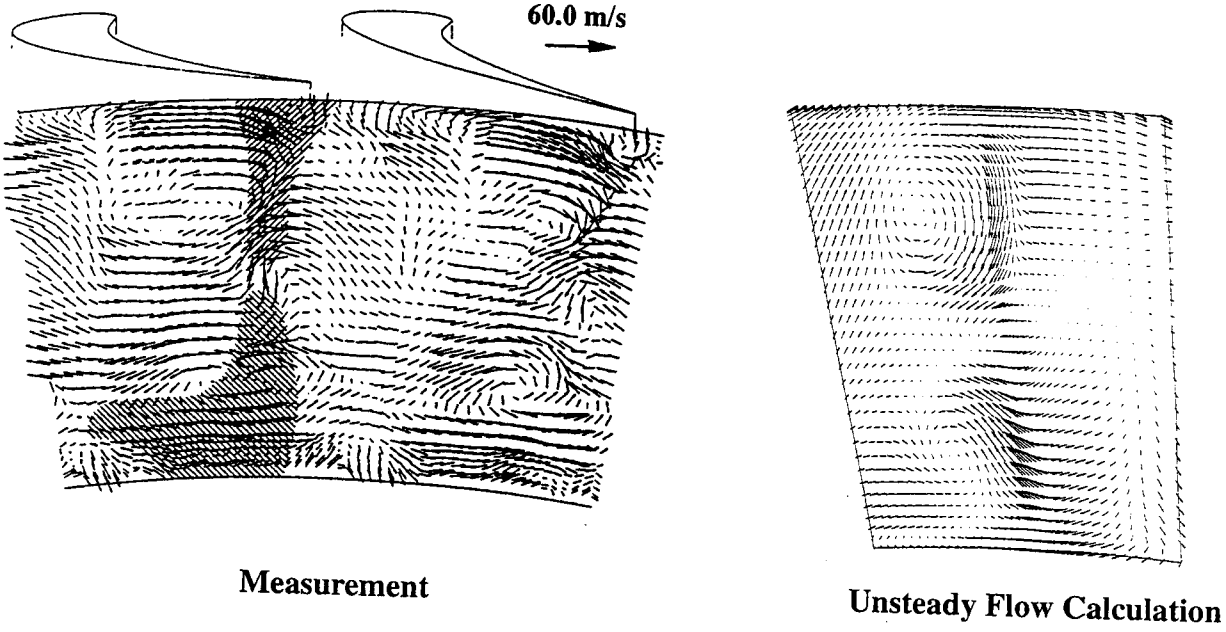

Fig. 13a. Comparison of secondary velocity vectors at rotor exit (Position 1).

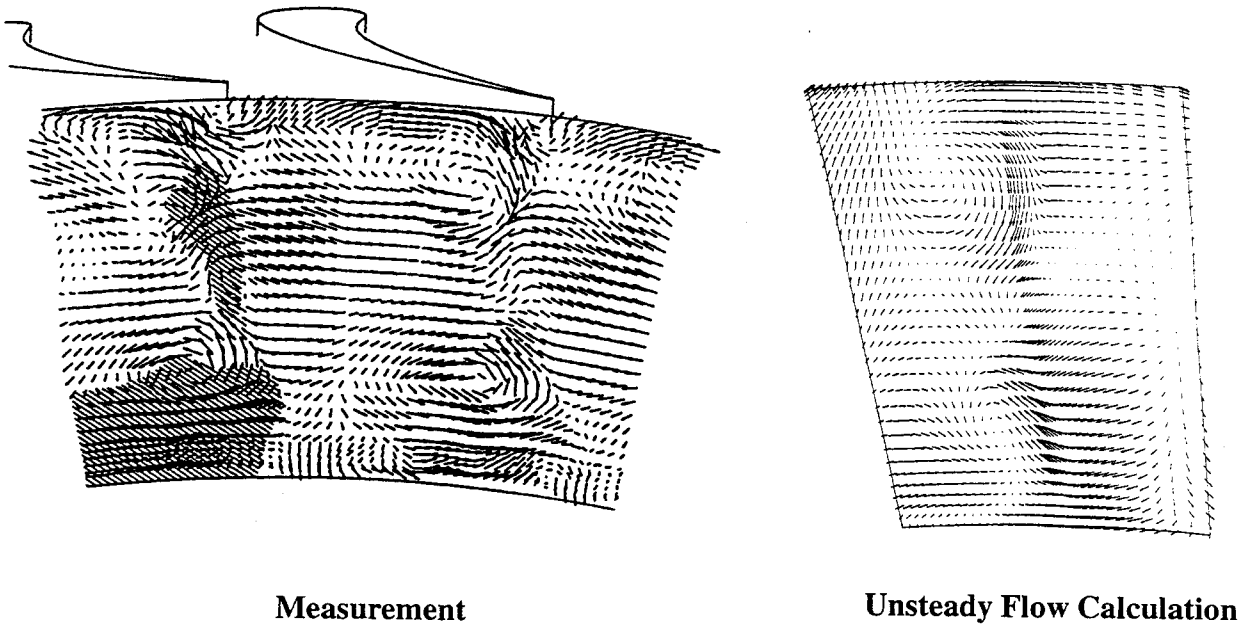

Fig. 13b. Comparison of secondary velocity vectors at rotor exit (Position 2).

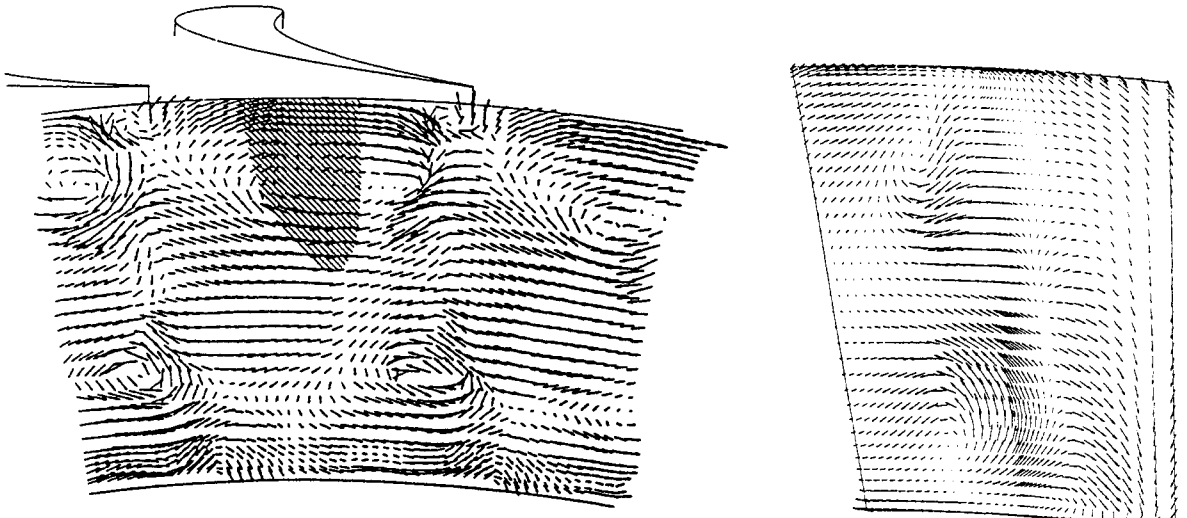

Measurement

Unsteady Flow Calculation

Fig. 13c. Comparison of secondary velocity vectors at rotor exit (Position 3).

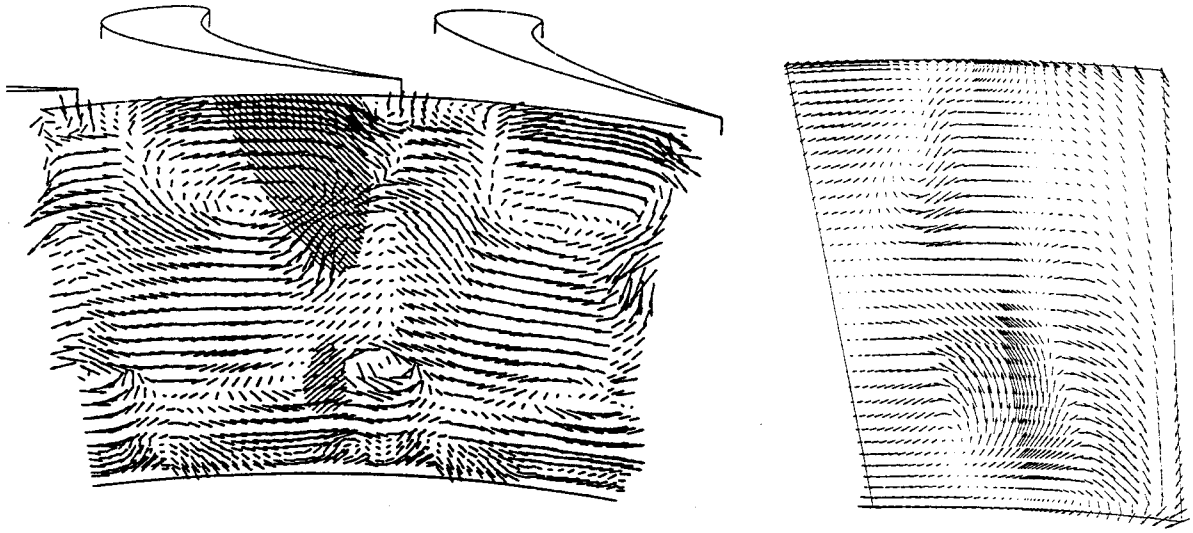

Measurement

Unsteady Flow Calculation

Fig. 13d. Comparison of secondary velocity vectors at rotor exit (Position 4).

The radial distribution of the stage exit flow angle is compared in Fig. 12. Numerical results based on a simple streamline curvature method are also presented in Fig. 12. The comparison in Fig. 12 is very good considering that the numerical results are based on the steady stage calculation. The only significant shortcoming of the numerical results occurs near the hub. This type of disagreement has also been previously observed in a similar analysis for the flow in a highly loaded turbine stage (for example, Schaub et al., 1993).

An unsteady flow calculation was conducted to investigate whether this discrepancy is due to the unsteady effects on the time-averaged flow field. The time-averaged results for the stator flow fields and the rotor blade loading from the unsteady calculation are virtually the same as those from the steady stage calculation. Instantaneous secondary velocity vectors at the exit of the rotor at four equally spaced times are shown in Fig. 13 for both the measurements and the calculation. The measured secondary velocity vectors are presented across two rotor blade passages while calculated results are for one rotor passage. Shaded areas in the measured results are regions with high turbulence intensity. The four rotor positions referenced in Fig. 13 are equally spaced by 20 percent of the stator pitch. The results from the unsteady calculation show that the center of the hub vortex has moved significantly away from the hub wall. This movement of the hub vortex is due to the interaction of the secondary flow that is coming out of the stator with the rotor flow field. In Fig. 14, the radial distribution of the stage exit angle is compared between the measurements and various prediction methods. Although the unsteady computation predicts the secondary flow field more accurately at the exit of the turbine stage, it requires about one hundred times more computing resources. Further refinements of the steady stage analysis methods should be made to improve the accuracy. The unsteady calculation results are being used for this purpose.

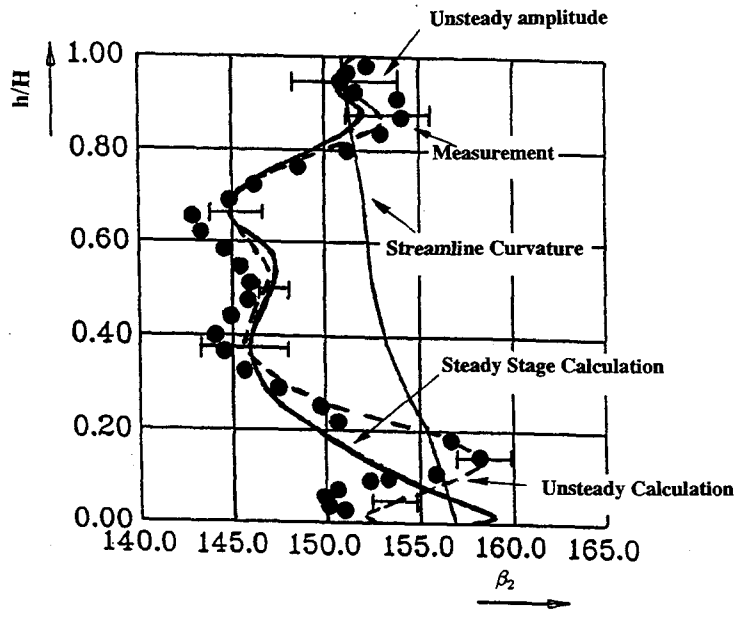

Fig. 14. Comparison of stage exit flow angle

CONCLUDING REMARKS

Detailed experimental and numerical studies have been performed to investigate the development of secondary flows and time-averaged flow characteristics in a single-stage, subsonic, axial turbine. Special attention was focused on examining how well a simple, steady multiple-blade-row calculation predicts time-averaged flow distributions at the exit of each blade row. The current study shows that the numerical method based on a simple steady state multiple-blade-row procedure calculates most of the time-averaged flow field accurately enough for design applications. However, the radial distribution of the flow angle at the exit of the stage was not properly calculated with the steady approach. The experimental study shows that the passage vortex near the hub of the rotor is transported toward the mid-span due to the unsteady interaction between the stator exit secondary flow and the rotor flow field. This interaction transports the hub vortex toward the mid-span in the time-averaged flow field. The steady stage calculation does not model this phenomenon. The unsteady flow calculation gives much better results for the time-averaged secondary flow field at the exit of the rotor and, consequently, the distribution of the stage exit flow angle. The current study indicates that accurate prediction of the secondary flows at the exit of the turbine stage requires numerical approaches which account for three-dimensional as well as unsteady effects. However, it seems that the three-dimensional effects, which can be modeled accurately with a steady multiple-blade-row calculation, are a primary mechanism in determining the time-averaged secondary flow field. The unsteady effects shift the passage vortex core away from the end wall. The cost of the unsteady flow analysis is about two orders of magnitude more than the steady flow analysis. Further research is necessary to improve the steady multiple-blade-row calculation method for practical design applications. The numerical results from the unsteady flow analysis can be used to improve the modeling of the steady stage calculation procedure.

REFERENCES

Arts, T., 1984, " Calculation of the 3D, Steady, Inviscid Flow in Transonic Axial Turbine Stages," ASME paper 84-GT-76.

Binder, A., 1985, " Turbulence Production due to Secondary Vortex Cutting in a Turbine Rotor ," Journal of Engineering for Gas Turbines and Power, Vol. 107, pp. 1039-1046.

Chien, K.Y., 1982, "Prediction of Channel and Boundary-Layer Flows With a Low Reynolds Number Turbulence Model," AIAA Journal Vol.20,No.1,pp. 33-38.

Copenhaver, W. W., Hah, C., and Puterbauch, S. L., 1993 " Three-Dimensional Flow Phenomena in a Transonic, High-Through-Flow Compressor Stage ," ASME Journal of Turbomachinery, Vol.115,No.2,pp.240-248.

Davis, R.L., Hobbs, D.E., and Weingold, H.D., 1988, "Prediction of Compressor Cascade Performance Using a Navier-Stokes Tchnique," ASME Journal of Turbomachinery, Vol.110,No.4.pp. 520-531.

Dawes, W.N., 1986, "Development of a 3D Navier-Stokes Solver for Application to All Types of Turbomachinery," ASME paper 86-GT-70.
Denton, J.D., 1986, "The Use of a Distributed Body Force to Simulate Viscous Flow in 3D flow Calculations," ASME Paper 86-GT-144.
Denton, J.D. and Singh, U.K., 1979, " Time Marching Methods for Turbomachinery Flow Calculation," VKI Lecture Series, 1979-7.
Dring, R.P. and Spear, D.A., " The Effects of Wake Mixing on Compressor Aerodynamics," ASME paper 90-GT-132.
Dring, R.P., Joslyn, H.D., Hardin, L.W. and Wagner, J.H., 1982, " Turbine Rotor-Stator Interaction ," ASME paper 82-GT-3.
Gallus, H.E., Groillus, H., and Lambertz, J., 1982, " The Influence of Blade Number Ratio and Blade Row Spacing on Axial-Flow Compressor Stator Blade Dynamic Load and Stage Sound Pressure Level ," ASME Journal of Engineering for Power,, Vol. 104, pp.633-644.
Giles, M.B., 1988, "Stator/Rotor Interaction in a Transonic Turbine," AIAA Paper 88-3093.
Hah, C., 1984, "A Navier-Stokes Analysis of Three-Dimensional Turbine Flows inside Turbine Blade Rows at Design and Off-Design Conditions," ASME Journal of Engineering for Gas Turbines and Power, Vol.106,No.2,pp.421-429.
Hah, C., 1986, "A Numerical Modeling of Endwall and Tip-Clearance Flow of an Isolated Compressor ," ASME Journal of Engineering for Gas Turbines and Power, Vol.108,No.1,pp.15-21.
Hah, C., 1987, "Calculation of Three-Dimensional Viscous Flows in Turbomachinery With an Implicit Relaxation Method," AIAA Journal of Propulsion and Power, Vol.3,No.5,pp.415-422.
Hah, C., Copenhaver, W. W., and Puterbauch, S. L., 1993 " Unsteady Aerodynamic Flow Phenomena in a Transonic Compressor Stage ," AIAA paper AIAA-93-1868.
Hah, C., and Wennerstrom, A.J., 1990, "Three-Dimensional Flowfields Inside a Transonic Compressor with Swept Blades," ASME Paper 90-GT-359.
Hodson, H.P., 1985, " Measurements of Wake-Generated Unsteadiness in the Rotor Passage of Axial Flow Turbines ," J. of Power, Vol.107, pp.466-477.
Hunter, I.H., 1982, " Endwall Boundary Layer Flows and Losses in an Axial Turbine Stage ," ASME Transaction J. of Power, Vol.104, pp.184-193.
Kerrebrock, J.L. and Mikolajczak, A.A., 1970, "Intra-Stator Transport of Rotor Wakes and Its Effect on Compressor Performance ," ASME Journal of Engineering for Power,Oct.,pp.359-368.
Meyer, R.X., 1958, " The Effect of Wakes on the Transient Pressure and Velocity Distributions in Turbomachines ," Transaction Journal of Basic Engineering, Oct., pp.1544-1552.
Ni, R.H., 1989," Prediction of 3D Multi Stage Turbine Flow Field Using a Multiple Grid Euler Solver," AIAA paper 89-0203.
Schaub, U.W., Vlasic, E. and Moustapha, S.H., 1993," Effect of Tip Clearance on the Performance of a Highly Loaded Turbine Stage ," Proceeding of AGARD PEP 82nd Symposium.
Utz, C., 1972," Experimentelle Untersuchung der Stromungsverluste in einer Mehrstufigen Axial-Turbine ," Thesis ETH Zurich.
Zeschky, J. and Gallus, H.E., 1993," Effects of Stator Wakes and Spanwise Nonuniform Inlet Conditions on the Rotor Flow of an Axial Turbine Stage," Transactions of the ASME, Vol. 115, pp.128-136.